

## van der Waals forces stabilize low-energy polymorphism in $B_2O_3$ : Implications for the crystallization anomaly

Guillaume Ferlat,<sup>1</sup> Maria Hellgren,<sup>1</sup> François-Xavier Coudert,<sup>2</sup> Henri Hay,<sup>1</sup> Francesco Mauri,<sup>1,3</sup> and Michele Casula<sup>1</sup>

<sup>1</sup>*Sorbonne Université, MNHN, UMR CNRS 7590, IRD, IMPMC, F-75005 Paris, France*

<sup>2</sup>*Chimie ParisTech, PSL University, CNRS, Institut de Recherche de Chimie Paris, 75005 Paris, France*

<sup>3</sup>*Dipartimento di Fisica, Università di Roma La Sapienza, Piazzale Aldo Moro 5, I-00185 Roma, Italy*



(Received 13 December 2018; published 10 June 2019)

The cohesive energies and structural properties of recently predicted, and never synthesized,  $B_2O_3$  polymorphs are investigated from *first principles* using density functional theory and high-accuracy many-body methods, namely, the random phase approximation and quantum Monte Carlo. We demonstrate that the van der Waals forces play a key role in making the experimentally known polymorph ( $B_2O_3$ -I) the lowest in energy, with many competing metastable structures lying only a few kcal/mol above. Remarkably, all metastable crystals are comparable in energy and density to the glass, while having anisotropic and mechanically soft structures. Furthermore, the best metastable polymorph according to our stability criteria has a structural motif found in both the glass and a recently synthesized borosulfate compound. Our findings provide a framework for understanding the  $B_2O_3$  anomalous behavior, namely, its propensity to vitrify in a glassy structure drastically different from the known crystal.

DOI: [10.1103/PhysRevMaterials.3.063603](https://doi.org/10.1103/PhysRevMaterials.3.063603)

### I. INTRODUCTION

Diboron trioxide ( $B_2O_3$ ) not only is the second most used component of industrial glasses after silica ( $SiO_2$ ), but also a canonical network-forming system *per se* (see, e.g., Refs. [1,2] for reviews). The originality of the low-pressure  $B_2O_3$  networks, either crystalline or vitreous, stems from their building blocks, which are bidimensional (2D) trigonal ( $BO_3$ ) units. This is in contrast with most network formers, such as silica, based on three-dimensional (3D) tetrahedral units. Fully 3D networks are then formed by binding these rigid units through flexible cation-oxygen-cation bonds, which give  $B_2O_3$  low-density structures, and a great potential for polymorphic transformations, under, e.g., high temperature or pressure. This is clearly reflected by various studies showing polyamorphic transformations in the glass [3–7] and to a lesser extent in the liquid [8,9].

However, our knowledge of the  $B_2O_3$  crystalline forms remains very limited: up to now, only one low-pressure  $BO_3$ -based crystal ( $B_2O_3$ -I) has been experimentally characterized [10] in addition to a high-pressure phase ( $B_2O_3$ -II), based upon  $BO_4$  tetrahedral units. The possible existence of another low-density polymorph, of unidentified structure, has been reported long ago [11], but the status of this report remains unclear since subsequent attempts failed to reproduce it. This is in sharp contrast with the rich polymorphism found in other oxide systems: in silica [12], for instance, more than 20 low-pressure polymorphs (from coesite to zeolites) built upon the same basic units have been experimentally reported.

Another striking and very uncommon feature is the *abnormal structural dissimilarity* between the glassy (*g*- $B_2O_3$ ) and crystalline forms. In *g*- $B_2O_3$ , about half of the  $BO_3$  elemental bricks are arranged into superstructural units, i.e., threefold rings referred to as boroxol rings [13,14],

fully absent from  $B_2O_3$ -I (see Fig. 1). As a consequence, the glass density is considerably smaller ( $\sim -30\%$ ) than the  $B_2O_3$ -I one. Likely related [15] but yet not understood, is the extremely high glass-forming ability of  $B_2O_3$ , arguably the best glass former. Indeed, the  $B_2O_3$ -I crystallization has never been observed from ambient pressure liquid, even if seeded with germs for months. The synthesis requires cooling the liquid under pressure, or alternatively using chemical routes, a behavior which has been coined as the *crystallization anomaly* [16].

Mostly inspired by the structural differences between *g*- $B_2O_3$  and  $B_2O_3$ -I, several theoretical works have predicted additional polymorphs [17–20]. In particular, a set of 25 new crystals [19], further complemented by two additional ones [20], has recently been obtained using density functional theory (DFT). It spans a very narrow energy range (a few kcal/mol), with values comparable to, or even lower than,  $B_2O_3$ -I, therefore challenging it as the ground state. Hence, high-level theories are needed to go beyond the standard approximations [local-density approximation (LDA), generalized gradient approximation (GGA)] that have been used in all previous DFT works. As a matter of fact, a drastically different physical picture emerges from our high-level calculations as will be shown later.

In the current work, we employ accurate many-body methods such as quantum Monte Carlo (QMC) and the random-phase approximation (RPA) to provide a definitive answer to the relative stability between  $B_2O_3$ -I and a subset of predicted polymorphs. In addition, we present results for a large set of polymorphs at different levels of DFT which demonstrate a huge effect of the van der Waals (vdW) forces on both the structures and energetics, an effect that has been neglected in all previous studies [17–20]. We definitely assess  $B_2O_3$ -I as the ground state while we introduce a polymorph (T0-0.5b),

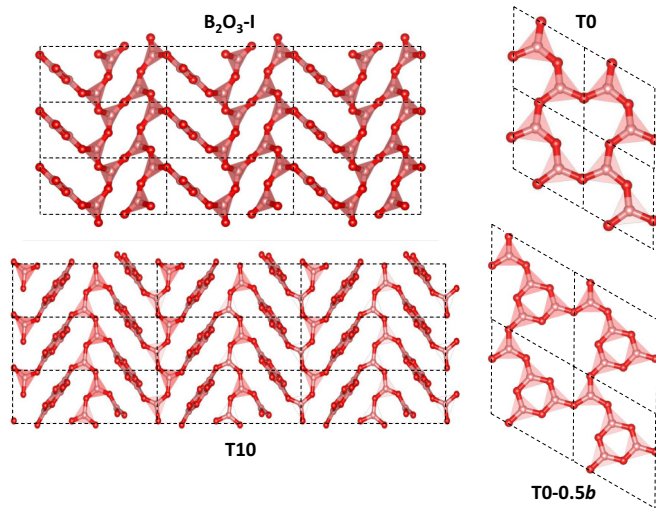


FIG. 1. Left:  $3 \times 3 \times 3$  supercell of  $B_2O_3$ -I and T10 seen in the  $(a, c)$  plane. Right: layers of T0 and T0-0.5b, the latter based on a mixed decoration of  $BO_3$  triangle and boroxol units. All the polymorphs considered in this work are 3D networks with the exception of T0, T0-0.5b, and T0-b, which are layered structures.

adapted from a recently synthesized borosulfate structure [21] which we reveal as the most stable among all putative structures. Its layers are decorated by triangle and boroxol units (Fig. 1) in equal proportions (1:1), making it a close, albeit crystalline, structural approximant of the glass.

## II. METHODS

Highly accurate QMC simulations have been carried out on three polymorphs ( $B_2O_3$ -I and two predictions T0 and T10). We used a Jastrow-Slater variational wave function, with Slater and Jastrow parts developed on a localized Gaussian basis set. The Jastrow factor contains correlation terms up to the four-body (electron-ion-electron-ion) form, able to capture van der Waals effects within variational Monte Carlo (VMC) [22]. The wave function has been fully optimized (Slater orbitals together with Jastrow coefficients) by energy minimization [23], starting from DFT-LDA generated one-body orbitals. Moreover, we have performed a complete structural relaxation for both cell parameters and internal coordinates at the VMC level [24]. Then, using relaxed VMC geometries, we have carried out lattice-regularized diffusion Monte Carlo simulations [25,26] and a very accurate finite-size extrapolation [27] in order to provide energies with accuracy better than 1.0 kcal/mol. A careful convergence of all relevant criteria, i.e., basis set, geometry, finite-size effects, and level of theory, is necessary, given the phase-space proximity of the  $B_2O_3$  polymorphs. All QMC calculations have been performed using the TURBORVB code [28]. Further details can be found in the Supplemental Material (SM) [29].

Calculations with the RPA were performed on a larger set of six polymorphs ( $B_2O_3$ -I, T0, T10, T3, T0-0.5b, and T0-b). The RPA is a state-of-the-art density functional approach based on many-body perturbation theory and the adiabatic connection fluctuation-dissipation formula [30,31]. By including polarization diagrams to infinite order in the Coulomb

interaction the RPA captures vdW forces [32,33]. It also provides an accurate description of Hartree-Fock exchange, and an overall good description of correlation effects (at least as far as energy differences are concerned). RPA total energies were calculated with the VASP code [34,35]. Computational details can be found in the SM [29].

Dispersive interactions can also be added in a semiempirical form to standard DFT approximations such as in the DFT-D approaches: for instance, in D2 [36] the vdW interaction coefficients ( $C_6$ ) are fixed for a given atomic pair while in the Tkatchenko-Scheffler (TS) approach [37], they are calculated self-consistently according to the atomic neighborhood. At a more advanced level, vdW are accounted for in fully nonlocal functionals that include polarization effects from first principles, such as in the vdW-DFT class of functionals [38,39]. In this work, we used representative functionals from these different levels, namely, D2 [36], TS [37] [added on top of the Perdew-Burke-Ernzerhof (PBE) functional [40], using the CASTEP code [41]], and the recently derived DF-cx [39] vdW-DFT functional (using the QUANTUM ESPRESSO package [42]). We checked explicitly that the use of different codes and pseudopotentials does not affect the reported results (Fig. S1 of the SM [29]). We also report results from LDA and GGA (PBE) functionals as references. In particular, the comparison between GGA and dispersion-corrected schemes (D2 and TS) built upon the same GGA, allows one to probe straightforwardly the relevance of vdW interactions. Thanks to the low computational cost of DFT, we studied a total of 27 polymorphs (those from Ref. [19] supplemented with T0-0.5b), which contain up to 135 atoms per unit cell [19].

Finally, we studied the mechanical properties via DFT-D2 calculations of second-order elastic constant tensors following a methodology described elsewhere [43,44]. See the SM for all the details of the DFT calculations [29].

## III. RESULTS AND DISCUSSION

We first assess the quality of the structural results obtained from the different schemes by relaxing the  $B_2O_3$ -I structure, and taking the experimentally known geometry as reference (Fig. 2). Not surprisingly, the lattice parameters obtained with LDA are underestimated (and the density overestimated by +6%), while the opposite is true for PBE (density error of -10%). This reflects the well-documented tendencies [45,46]

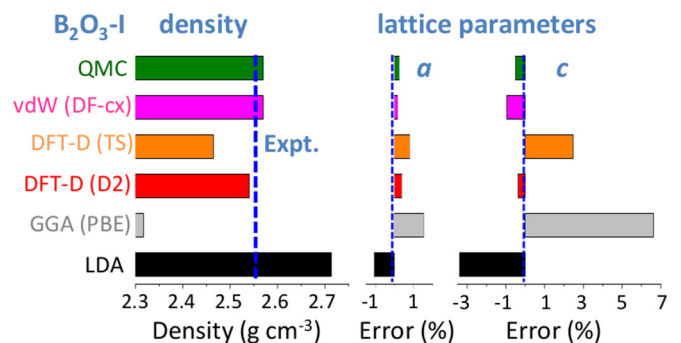


FIG. 2. Density and lattice parameters of  $B_2O_3$ -I from different *ab initio* schemes. Errors on lattice parameters are expressed relatively to the experimental values.

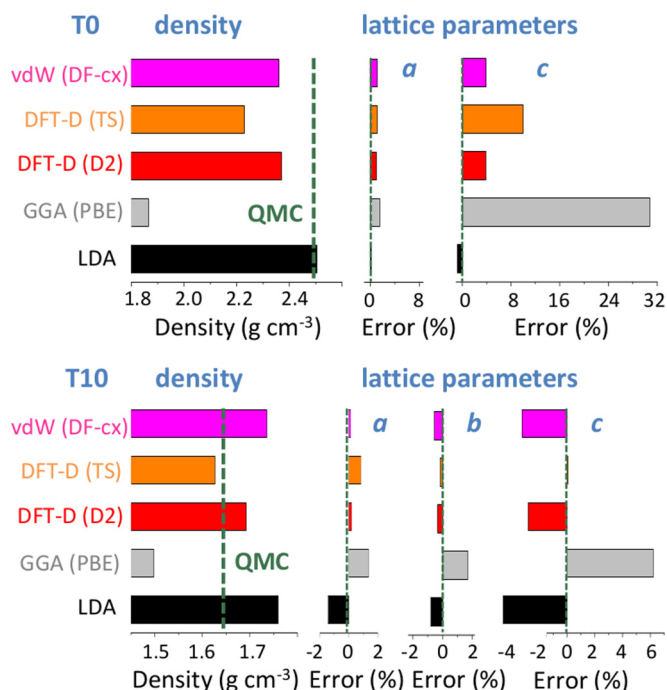


FIG. 3. Density and lattice parameters of T0 and T10 from different *ab initio* schemes. Errors on lattice parameters are expressed relatively to the QMC values.

of LDA to overbind and of PBE to underbind. Note, however, that the size of these errors is large for a nonlayered inorganic system, placing  $B_2O_3$ -I in the topmost range (95th percentile) of volume errors for inorganic materials of the Materials Project database [47]. Interestingly, these deficiencies are largely cured not only by QMC (+0.5% error on density) but also by all the vdW-corrected schemes used here, which show a systematic improvement.

Although  $B_2O_3$ -I is a fully connected 3D network made of strong interatomic bonds, the importance of the vdW corrections stems from the structural porosity, arising from *locally planar* regions—on the scale of a few building units—arranged in a *zigzag* pattern thanks to the B-O-B angular flexibility (Fig. 1). This leads to a *softer* direction, perpendicular to the locally planar regions, and nearly parallel to the *c* direction, as reflected by larger errors in this lattice parameter (Fig. 2). The existence of such a softer direction is found in all but two polymorphs (see also Fig. 3).

We now focus on the densities and energies of two previously predicted [19] polymorphs, namely, T0 and T10 using QMC results as reference in the absence of experimental data. We report these results in Figs. 3 and 4. In the following, all crystals' energies are expressed with respect to the  $B_2O_3$ -I one. Similarly to the experimentally known case, PBE severely underestimates the densities. This impacts the energies, which are also underestimated. Note that T10, which in the PBE original predictions [19] had a slightly lower energy ( $\sim -1$  kcal/mol) than  $B_2O_3$ -I, turns out to be metastable ( $\sim +3$  kcal/mol). On the contrary, the vdW-corrected DFT schemes perform reasonably well in both densities and energies. Moreover, the RPA energies agree well with QMC (Fig. 4, right panel).

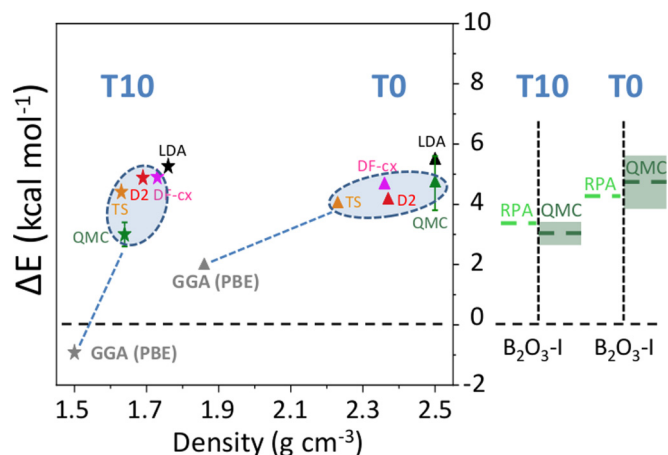


FIG. 4. Left: energies, relative to  $B_2O_3$ -I, from the different schemes for two predicted polymorphs, T0 (triangles) and T10 (stars). The blue-shaded ellipses encompass vdW-corrected results. Right: RPA and QMC energies compared. The green-shaded rectangles correspond to the QMC error bars.

We also calculated RPA energies for the T0-0.5*b*, T0-*b*, and T3 structures, shown in Fig. 5 together with those from the different DFT schemes. We note that all three vdW-corrected functionals yield essentially the same results, with a typical variability of 2 kcal/mol on the energies, and compare well with the more advanced RPA. This gives strong confidence in the overall picture. A complete account for the full set of 27  $B_2O_3$  polymorphs, using the various DFT frameworks, is reported (Fig. S2) in the SM [29]. In the following we shall

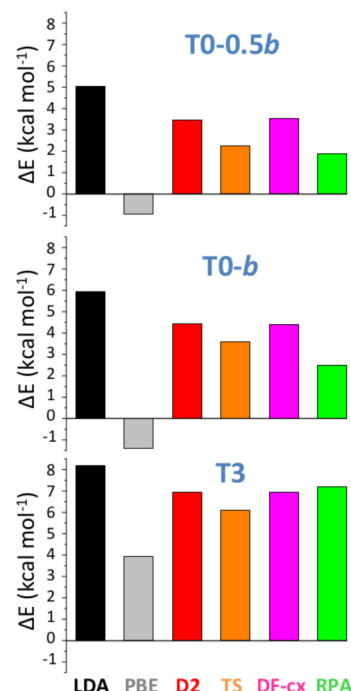


FIG. 5. Energies, relative to  $B_2O_3$ -I (in kcal mol<sup>-1</sup>) obtained from the different *ab initio* schemes, including RPA, for three polymorphs (T0-0.5*b*, T0-*b*, and T3). The energies for T0 and T10 are reported in Fig. 4.

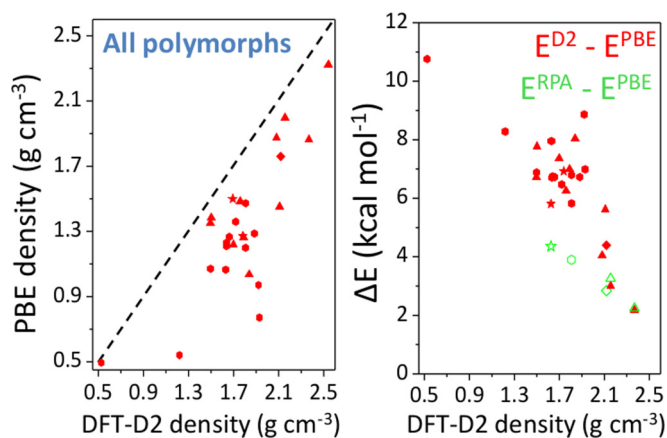


FIG. 6. Corrections to the PBE density (left panel) and relative energy (right panel) brought back by the vdW-corrected schemes, using DFT-D2 (red) or RPA (green symbols).

take D2 as representative of the vdW-corrected functionals [48], in order to make a thorough comparison with PBE, and show the impact of the dispersive interactions on the B<sub>2</sub>O<sub>3</sub> polymorphism.

Figure 6 highlights the density and energy corrections brought back by the vdW contributions. Being attractive, the vdW forces systematically provide denser structures (Fig. 6, left panel), on average by 40% and by up to 150% for some polymorphs, such as T8-*b*. Such high figures reflect the fact that for many polymorphs the vdW scheme allows one to find a qualitatively different geometry from the PBE one (e.g., internal voids and large-scale rings tend to be less symmetric and more puckered). This densification effect, which acts effectively as an internal negative pressure, results in an increasing enthalpic penalty with decreasing density (Fig. 6, right panel). Overall, the more porous the polymorph,

the larger the vdW contribution to the energy. This trend is supported by the RPA results presented in the same figure, and is also in line with studies of, e.g., silica zeolites [46]. In other words, the energies of the predicted polymorphs are more impacted by vdW than the B<sub>2</sub>O<sub>3</sub>-I one, because of their lower density.

The energy diagram (Fig. 7, left panel) resulting from the vdW inclusion provides several major outcomes. First, all predicted polymorph energies fall above B<sub>2</sub>O<sub>3</sub>-I, while in the PBE picture [19,20] many polymorphs are possible candidates for the ground state. Note that the overall correlation between metastability and density is now in line with the one observed for silica polymorphs [43]. Although the results are presented at 0 K, we checked that the picture obtained at 300 K is unchanged within 1 kcal/mol (by computing finite-temperature contributions to the vibrational free energy within the DFT-D2 scheme; see the SM [29]). A second important point is that, despite being metastable, most of the predicted polymorphs are still within a thermodynamically accessible energy range, estimated at ~7 kcal/mol [49]. In particular, polymorphs such as T0-0.5*b* and T0-*b* could be amenable to synthesis. Remarkably, the layers that constitute these polymorphs are found experimentally in several chemically complex borates [21,50,51].

However, assessing the synthesizability of a given polymorph is a very challenging task, since the energy is not the sole ingredient at play. Following an earlier work on silica zeolites which associated experimentally observed structures with good mechanical properties [43], we undertook a comprehensive characterization of the mechanical properties of the B<sub>2</sub>O<sub>3</sub> polymorphs, including bulk (*B*), Young (*E*), and shear (*G*) moduli as well as linear compressibility and Poisson’s ratio [44]. In all the calculated moduli, and as illustrated in Fig. 7 (right panel) for the bulk modulus, there is a rather clear distinction between B<sub>2</sub>O<sub>3</sub>-I (*B* ~ 60 GPa) and most

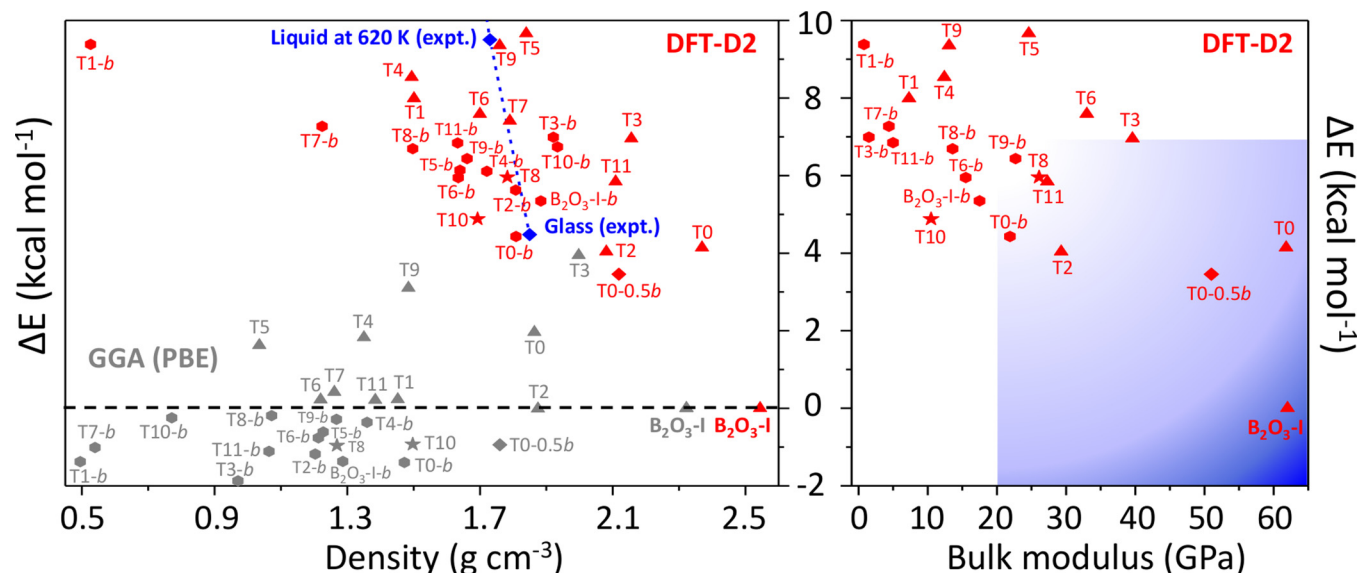


FIG. 7. Left: Energy, relative to B<sub>2</sub>O<sub>3</sub>-I, and density for all polymorphs using DFT-D2 (red) and PBE (gray symbols). Symbols refer to the relative proportions of structural units (triangles:boroxol) in the polymorphs: Δ only BO<sub>3</sub> triangles (1:0), ○ only boroxol rings (0:1), ☆ mixed decoration (3:1), ◇ mixed decoration (1:1). Experimental data (liquid and glass) are from Ref. [52]. Right: energy and bulk modulus using DFT-D2. The inner rectangle schematically represents the *feasibility* window.

of the other polymorphs which show much smaller values ( $\sim 0$ – $30$  GPa). For illustrative purposes, the shaded-blue rectangle in the energy-versus- $B$  parameter space delimits the ranges of values in experimentally realized silica polymorphs. Noticeably, this area excludes most of the predicted  $B_2O_3$  polymorphs, with a few noticeable exceptions including T0- $b$  and T0-0.5 $b$ .

Further, for most polymorphs,  $E$  and  $G$ , which are directional quantities, show high anisotropies, implying that there is one direction much *weaker* than the others with respect to an applied stress. This is in line with the aforementioned *soft* direction in these structures. In silica zeolites [43], proposals of *feasibility* criteria were derived from the lowest values of these mechanical quantities: strictly transferring these criteria [53] to  $B_2O_3$  leaves only  $B_2O_3$ -I as a realizable structure with, however, a handful of additional candidates (T3, T11,  $B_2O_3$ -I- $b$ , T0, and T0-0.5 $b$ ) close to the criteria thresholds. Thus, many of the predicted structures suffer from mechanical stability issues and this may be one of the reasons why they have not been experimentally realized yet.

Our findings have strong implications for understanding the  $B_2O_3$  behavior at the glass transition. Indeed, the vast majority of the predicted polymorphs are clustered close to the liquid and glass states in the energy-density diagram (dashed-blue line in Fig. 7, left panel). Since the glass structure is generally expected to resemble that of the underlying crystals, Fig. 7 provides a framework to understand the glass state and its apparent anomalous properties, such as its low density, its high fraction of rings, and its strong structural dissimilarity with  $B_2O_3$ -I. In addition, the existence of many competing polymorphs of similar energies, as observed here, has been shown to correlate with the glass-forming ability; a situation reported for a large range of systems [54,55] and in various models [56–58].

These aspects, which combine the energetics with the mechanical properties, allow one to propose the following explanation for the  $B_2O_3$  *crystallization anomaly*. As the low-density liquid is cooled and gets closer to the region of high polymorphic degeneracy, it hovers over a rugged energy landscape, i.e., dominated by many local minima of similar energies. These minima are associated to low-density and mechanically weak structures prone to collapse into an amorphous framework. Although there exists a ground state ( $B_2O_3$ -I) of higher density, the driving force (energy separation between the metastable states and  $B_2O_3$ -I) is small enough and the energy barriers (associated to the topological

reconfiguration required to reach the  $B_2O_3$ -I density) are sufficiently high so that the system is kinetically trapped, in accordance with the very sluggish kinetics found in this system [15]. Applying pressure to the melt favors higher density and stiffer structures in the energy landscape, and thus results in the  $B_2O_3$ -I crystallization.

#### IV. CONCLUSIONS

We have revealed that  $B_2O_3$  is a system remarkably sensitive to vdW interactions in both energies and structures. The importance of vdW in  $B_2O_3$  is striking and unexpected, particularly when compared to  $SiO_2$ , a system commonly considered similar for which, however, only mild effects from vdW have been reported [46]. Thus, the set of polymorphs studied in this work constitutes a valuable test bed to develop new methods for the accurate treatment of electronic correlation. At the same time, the account of vdW allows one to retrieve a polymorphic picture which not only supports the generally admitted experimental knowledge ( $B_2O_3$ -I is the ground state) but also brings the metastable polymorphs closer to the glass in the energy-density phase space. From the simultaneous characterization of energies and mechanical properties carried out here, we provide a semiquantitative map of the *likeliness of synthesizability*. Not only is it in agreement with the experimental observations—the structural motif from the most robust predicted polymorph (T0-0.5 $b$ ) has been found in synthesized borates—but also it provides a fundamental framework to explain the  $B_2O_3$  intriguing anomalies. The glass has a low density and a high amount of boroxol rings because the supercooled liquid acquires those structural characteristics from the closest underlying crystalline polymorphs. It, however, fails to crystallize in any of these because of their weak mechanical properties.

#### ACKNOWLEDGMENTS

We thank H. Hillebrecht for communicating the results of Ref. [21] prior to their publication. This work was performed using HPC resources from GENCI-TGCC/CINES/IDRIS (Grants No. A0030906493, No. A0030801875, No. A0010906493, and No. A0010907625) and from PRACE (project 2016143322). Financial support from the French National Research Agency program PIPOG ANR-17-CE30-0009 and from the program Emergence-Ville de Paris are acknowledged.

- 
- [1] G. Ferlat, *Rings in Network Glasses: The  $B_2O_3$  Case* (Springer, Switzerland, 2015), Chap. 14, p. 367.
- [2] A. C. Wright, *Phys. Chem. Glasses: Eur. J. Glass Sci. Technol., Part B* **59**, 65 (2018).
- [3] J. Nicholas, S. Sinogeikin, J. Kieffer, and J. Bass, *Phys. Rev. Lett.* **92**, 215701 (2004).
- [4] S. K. Lee, K. Mibe, Y. Fei, G. D. Cody, and B. O. Mysen, *Phys. Rev. Lett.* **94**, 165507 (2005).
- [5] K. Trachenko, V. V. Brazhkin, G. Ferlat, M. T. Dove, and E. Artacho, *Phys. Rev. B* **78**, 172102 (2008).
- [6] A. Zeidler, K. Wezka, D. A. J. Whittaker, P. S. Salmon, A. Baroni, S. Klotz, H. E. Fischer, M. C. Wilding, C. L. Bull, M. G. Tucker, M. Salanne, G. Ferlat, and M. Micoulaut, *Phys. Rev. B* **90**, 024206 (2014).
- [7] S. K. Lee, Y.-H. Kim, P. Chow, Y. Xiao, J. Cheng, and G. Shen, *Proc. Natl. Acad. Sci. USA* **115**, 5855 (2018).
- [8] V. V. Brazhkin, I. Farnan, K. I. Funakoshi, M. Kanzaki, Y. Katayama, A. G. Lyapin, and H. Saitoh, *Phys. Rev. Lett.* **105**, 115701 (2010).
- [9] O. L. G. Alderman, G. Ferlat, A. Baroni, M. Salanne, M. Micoulaut, C. J. Benmore, A. Lin, A. Tamaloni, and J. K. R. Weber, *J. Phys.: Condens. Matter* **27**, 455104 (2015).
- [10] G. E. Gurr, P. W. Montgomery, C. D. Knutson, and B. T. Gorres, *Acta Crystallogr.* **B26**, 906 (1970).

- [11] S. S. Cole and N. W. Taylor, *J. Am. Ceram. Soc.* **18**, 55 (1935).
- [12] P. M. Piccione, C. Laberty, S. Yang, M. A. Cambor, A. Navrotsky, and M. E. Davis, *J. Phys. Chem. B* **104**, 10001 (2000).
- [13] R. E. Youngman, S. T. Haubrich, J. W. Zwanziger, M. T. Janicke, and B. F. Chmelka, *Science* **269**, 1416 (1995).
- [14] P. Umari and A. Pasquarello, *Phys. Rev. Lett.* **95**, 137401 (2005).
- [15] E. D. Zanotto and D. R. Cassar, *Sci. Rep.* **7**, 43022 (2017).
- [16] D. R. Uhlmann, J. F. Hays, and D. Turnbull, *Phys. Chem. Glasses* **8**, 1 (1967).
- [17] A. Takada, C. R. A. Catlow, and G. D. Price, *Phys. Chem. Glasses* **44**, 147 (2003).
- [18] L. Huang, M. Durandurdu, and J. Kieffer, *J. Phys. Chem. C* **111**, 13712 (2007).
- [19] G. Ferlat, A. P. Seitsonen, M. Lazzeri, and F. Mauri, *Nat. Mater.* **11**, 925 (2012).
- [20] F. Claeysens, J. N. Hart, N. C. Norman, and N. L. Allan, *Adv. Funct. Mater.* **23**, 5887 (2013).
- [21] M. Daub and H. Hillebrecht, *Eur. J. Inorg. Chem.* **2015**, 4176 (2015).
- [22] S. Sorella, M. Casula, and D. Rocca, *J. Chem. Phys.* **127**, 014105 (2007).
- [23] C. J. Umrigar, J. Toulouse, C. Filippi, S. Sorella, and R. G. Hennig, *Phys. Rev. Lett.* **98**, 110201 (2007).
- [24] M. Barborini, S. Sorella, and L. Guidoni, *J. Chem. Theory Comput.* **8**, 1260 (2012).
- [25] M. Casula, C. Filippi, and S. Sorella, *Phys. Rev. Lett.* **95**, 100201 (2005).
- [26] M. Casula, S. Moroni, S. Sorella, and C. Filippi, *J. Chem. Phys.* **132**, 154113 (2010).
- [27] M. Dagrada, S. Karakuzu, V. L. Vildosola, M. Casula, and S. Sorella, *Phys. Rev. B* **94**, 245108 (2016).
- [28] S. Sorella, Turborvb, quantum Monte Carlo software for electronic structure calculations, <http://people.sissa.it/sorella/web/>.
- [29] See Supplemental Material at <http://link.aps.org/supplemental/10.1103/PhysRevMaterials.3.063603> for computational details and additional data, which includes Refs. [60–72].
- [30] D. C. Langreth and J. P. Perdew, *Solid State Commun.* **17**, 1425 (1975).
- [31] O. Gunnarsson and B. I. Lundqvist, *Phys. Rev. B* **13**, 4274 (1976).
- [32] A. Marini, P. García-González, and A. Rubio, *Phys. Rev. Lett.* **96**, 136404 (2006).
- [33] S. Lebègue, J. Harl, T. Gould, J. G. Ángyán, G. Kresse, and J. F. Dobson, *Phys. Rev. Lett.* **105**, 196401 (2010).
- [34] G. Kresse and J. Furthmüller, *Phys. Rev. B* **54**, 11169 (1996).
- [35] G. Kresse and D. Joubert, *Phys. Rev. B* **59**, 1758 (1999).
- [36] S. Grimme, *J. Comput. Chem.* **27**, 1787 (2006).
- [37] A. Tkatchenko and M. Scheffler, *Phys. Rev. Lett.* **102**, 073005 (2009).
- [38] K. Lee, E. D. Murray, L. Kong, B. I. Lundqvist, and D. C. Langreth, *Phys. Rev. B* **82**, 081101(R) (2010).
- [39] T. Thonhauser, S. Zuluaga, C. A. Arter, K. Berland, E. Schröder, and P. Hyldgaard, *Phys. Rev. Lett.* **115**, 136402 (2015).
- [40] J. P. Perdew, K. Burke, and M. Ernzerhof, *Phys. Rev. Lett.* **77**, 3865 (1996).
- [41] S. J. Clark, M. D. Segall, C. J. Pickard, P. J. Hasnip, M. I. J. Probert, K. Refson, and M. C. Payne, *Z. Kristallogr.* **220**, 567 (2005).
- [42] P. Giannozzi, S. Baroni, N. Bonini, M. Calandra, R. Car, C. Cavazzoni, D. Ceresoli, G. L. Chiarotti, M. Cococcioni, I. Dabo *et al.*, *J. Phys.: Condens. Matter* **21**, 395502 (2009), <http://www.quantum-espresso.org>.
- [43] F.-X. Coudert, *Phys. Chem. Chem. Phys.* **15**, 16012 (2013).
- [44] H. Hay, Ph.D. thesis, Université Pierre & Marie Curie, Paris, 2016, <https://tel.archives-ouvertes.fr/tel-0147013a1>.
- [45] P. Haas, F. Tran, and P. Blaha, *Phys. Rev. B* **79**, 085104 (2009).
- [46] H. Hay, G. Ferlat, M. Casula, A. P. Seitsonen, and F. Mauri, *Phys. Rev. B* **92**, 144111 (2015).
- [47] W. Sun, S. T. Dacek, S. P. Ong, G. Hautier, A. Jain, W. D. Richards, A. C. Gamst, K. A. Persson, and G. Ceder, *Sci. Adv.* **2**, e1600225 (2016).
- [48] The calculation of the mechanical moduli (Fig. 7) is readily available in the CRYSTAL14 code [59] for D2 only (among vdW schemes).
- [49] For binary oxides, the range of observed polymorphs (as defined by the 90th percentile of a statistical analysis [47]) is 94 meV/atom, i.e., 10.8 kcal/(mol B<sub>2</sub>O<sub>3</sub>). Taking silica as a close parent system, the highest energy above quartz (among SiO<sub>2</sub> polymorphs for which calorimetric data are available) is 6.88 kcal/(mol 2SiO<sub>2</sub>) (ISV zeolite) [12].
- [50] M.-S. Wang, G.-C. Guo, W.-T. Chen, G. Xu, W.-W. Zhou, K.-J. Wu, and J.-S. Huang, *Angew. Chem., Int. Ed.* **46**, 3909 (2007).
- [51] M.-C. Liu, P. Zhou, H. G. Yao, S.-H. Ji, R.-C. Zhang, M. Ji, and Y.-L. An, *Eur. J. Inorg. Chem.* **2009**, 4622 (2009).
- [52] N. E. Shmidt, *Russ. J. Inorg. Chem.* **11**, 241 (1966).
- [53] Minimal value of the Young modulus  $E_{\min} \geq 20$  GPa and elastic anisotropy  $\eta \leq 5$ , where  $\eta = \max(\frac{E_{\max}}{E_{\min}}, \frac{G_{\max}}{G_{\min}})$ . However, the criterion on anisotropy likely does not apply to layered structures (T0, T0-0.5*b*, and T0-*b*).
- [54] E. Perim, D. Lee, Y. Liu, C. Toher, P. Gong, Y. Li, W. N. Simmons, O. Levy, J. J. Vlassak, J. Schroers *et al.*, *Nat. Commun.* **7**, 12315 (2016).
- [55] C. H. L. Goodman, *Nature (London)* **257**, 370 (1975).
- [56] G. G. Naumis, *Phys. Rev. E* **85**, 061505 (2012).
- [57] P. Ronceray and P. Harrowell, *Phys. Rev. E* **96**, 042602 (2017).
- [58] J. Russo, F. Romano, and H. Tanaka, *Phys. Rev. X* **8**, 021040 (2018).
- [59] R. Dovesi, R. Orlando, A. Erba, C. M. Zicovich-Wilson, B. Civalleri, S. Casassa, L. Maschio, M. Ferrabone, M. De La Pierre, P. D’Arco *et al.*, *Int. J. Quantum Chem.* **114**, 1287 (2014).
- [60] B. Winkler, C. J. Pickard, V. Milman, and G. Thimm, *Chem. Phys. Lett.* **337**, 36 (2001).
- [61] D. Vanderbilt, *Phys. Rev. B* **41**, 7892(R) (1990).
- [62] P. Richet, Y. Bottinga, L. Denielou, J. P. Petitet, and C. Tequi, *Geochim. Cosmochim. Acta* **46**, 2639 (1982).
- [63] F. Mouhat and F.-X. Coudert, *Phys. Rev. B* **90**, 224104 (2014).
- [64] R. Gaillac, P. Pullumbi, and F.-X. Coudert, *J. Phys. Condens. Matter* **28**, 275201 (2016).
- [65] M. Burkatzki, C. Filippi, and M. Dolg, *J. Chem. Phys.* **126**, 234105 (2007).
- [66] M. Casula, C. Attaccalite, and S. Sorella, *J. Chem. Phys.* **121**, 7110 (2004).

- [67] M. Marchi, S. Azadi, M. Casula, and S. Sorella, *J. Chem. Phys.* **131**, 154116 (2009).
- [68] N. Devaux, M. Casula, F. Decremps, and S. Sorella, *Phys. Rev. B* **91**, 081101(R) (2015).
- [69] M. Calandra Buonaura and S. Sorella, *Phys. Rev. B* **57**, 11446 (1998).
- [70] R. Assaraf and M. Caffarel, *J. Chem. Phys.* **119**, 10536 (2003).
- [71] C. Filippi and C. J. Umrigar, *Phys. Rev. B* **61**, R16291(R) (2000).
- [72] S. Sorella and L. Capriotti, *J. Chem. Phys.* **133**, 234111 (2010).